Experimental Study of Static and Fatigue Behavior of CFRP-Balsa Sandwiches under Three-point Flexural Loading

Sebastian Marian Zaharia,[a,*] Cristin Olimpiu Morariu,[a] Anisor Nedelcu,[a] and Mihai Alin Pop [b]

Balsa wood is a natural cellular material with an excellent resistance-to-weight ratio that is ideal for manufacturing the core of sandwich structures. In this study, sandwich specimens with a carbon-fiber-reinforced polymer (CFRP) skin and a balsa wood core were tested with static and dynamic loading. Three-point flexural tests in static regime determined the mechanical characteristics of the CFRP-balsa specimens that were needed for subsequent fatigue strength tests. Also, experimental research was performed on the Charpy impact response of the CFRP-balsa sandwich specimens. This study implemented an accelerated fatigue testing method to identify and predict the mean fatigue life of the CFRP-balsa sandwich specimens subjected to cyclic fatigue *via* three-point flexural tests. Using the accelerated fatigue and the three-point flexural testing methodology on the CFRP-balsa sandwich specimens, the testing period was reduced by 11.9 times, and thus the material costs necessary for the tests were also reduced. Also, the breaking surfaces were analysed to reveal the failure modes of CFRP-balsa specimens subjected to static and fatigue tests at three-point flexural and at impact tests.

Keywords: Balsa wood; CFRP; Sandwich structure; Three-point flexural test; Mean fatigue life; Accelerated fatigue test

*Contact information: a: Faculty of Technological Engineering and Industrial Management, Transylvania University of Brasov, Mihai Viteazu Street, No. 5, 500174, Brasov, Romania; b: Faculty of Materials Science and Engineering, Transylvania University of Brasov, Colina Universitatii Street, No. 1, 500084, Brasov, Romania; *Corresponding author: zaharia_sebastian@unitbv.ro*

INTRODUCTION

The composite sandwich structure is represented by a panel consisting of two face sheets (skins) that are bonded with an adhesive to a core that maintains the relative position of the two skins. Composite sandwich structures are complex structures with the following features: good specific mass properties (stiffness and strength), good thermal and sound insulation, good durability, good corrosion and fatigue resistance, easily repairable, and low water-absorption (Harris 2003; Li *et al.* 2014). Balsa wood provides good shear strength; low acquisition cost; high fatigue resistance; ease of manufacturing, processing, and assembly; and superior performance in energy absorption (Vinson 1999). Midgley *et al.* (2010) classified balsa wood according to density: light (80 kg/m^3 to 120 kg/m^3), medium (120 kg/m^3 to 180 kg/m^3), and heavy (180 kg/m^3 to 220 kg/m^3).

The sandwich structures analyzed in this paper are balsa wood core and carbon-fiber-reinforced polymer (CFRP) skin bonded with an adhesive film (Fig. 1). The advantages conferred by these sandwich structures with a balsa wood core render them

widely used in the aerospace, marine, building, renewable energies, rail, and road industries (Kotlarewski *et al*. 2014).

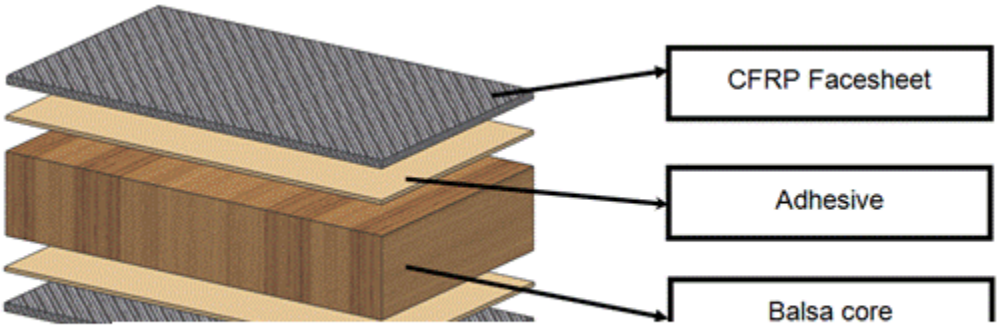

Fig. 1. The CFRP-Balsa sandwich structure

Sandwich structures with skins made of composite materials and various types of cores are intensively studied in specialized laboratories. Da Silva and Kyriakides (2007) performed an extensive study of the response to compression and the failure analysis of specimens taken from commercially available balsa wood and tested them in various directions (axial, radial, and tangential). The balsa wood subjected to axial compression, flexure, and torsion, indicated a linear increase of the modulus of elasticity and strength *versus* density. Those subjected to radial compression, the modulus of elasticity and strength varied non-linearly (Borrega and Gibson 2015). In a recent study (Toson *et al.* 2014), a complex model was developed to determine the response of balsa wood material subjected to different load types. To validate the proposed model, numerous experimental tests and finite element analyses were conducted to determine its performance.

To optimize the sandwich structures, materials (balsa/timber) with different densities are combined to obtain the greatest rigidity and strength. Discontinuities that occur when combining materials can cause sudden changes in the shear angles and local buckling in sandwich structures' skins, thus possibly introducing stress concentrators. To estimate the local stress concentrators, two analytical models were developed by Osei-Antwi *et al.* (2014) for butt and scarf joints of sandwich cores. Chen *et al.* (2011) proposed a dynamic method of explosion simulation using a crushing foam projectile launched by a gas gun with speeds between 30 m/s and 60 m/s. This experimental method was developed to determine the failure modes of the composite sandwich panels made of carbon-fiber skin and balsa wood core. Jover *et al.* (2014) investigated the composite sandwich structures with balsa core and carbon-fiber skin with single and multi-site sequential ballistic impacts. The experimental results led to a ballistic limit in the CFRP-balsa sandwich structure of 96 m/s^{-1}, which was capable of withstanding impact from small objects resulting from a blast, hurricane, tornado, and road and runway debris.

Recently, Kandare *et al*. (2014) evaluated the properties of the response to fire of flax/epoxy laminate and balsa-flax/epoxy sandwich composites by applying a heat flux of 50 kW/m^2. To improve these properties, a thin layer of glass fibers impregnated with ammonium polyphosphate was bonded to the surface of the composite. Atas and Sevim (2010) conducted an experimental investigation of the impact response and the failure modes of E-glass/epoxy skins and polyvinyl chloride (PVC) foam, and balsa wood cores used in the marine industry. As a result of the experimental tests on different impact

energies, they obtained load-deflection curves and energy profile diagrams. The failure modes that emerged (fiber fractures at upper and lower skins, delamination between glass-epoxy layers, core shear fractures, and face/core debonding) were analyzed using visual and destructive inspections of the tested structures. In operation, sandwich structures are subjected to various types of stress, such as compression, tensile, flexure, and impact. To assess the failures that occur during use, various stress conditions (static and dynamic), similar to those that result in operating mode, are tested in specialized laboratories. Chemami *et al*. (2012) studied the mechanical behavior and the lifetimes of 3-point bending in static and fatigue modes. The study was performed on two different composite sandwich laminates with fiberglass and epoxy resin skins with unidirectional reinforcements, and a core of PVC foam. As a result of the study, they concluded that the fracture surfaces revealed the different modes of damages that caused the material fracture. Boukharouba *et al*. (2014) proposed the experimental analysis and modelled the fatigue performances of sandwich structures made from CFRP skin and a Nomex core, using the three-point bending test with different levels of loading. The results obtained experimentally showed that the evolution of damage during the fatigue loading of sandwich structures, as well as the delamination between the top skin and the core, caused failure to the structure. Abbadi *et al.* (2010) studied the four-point flexural test behavior of honeycomb composite core (aramid fiber) sandwich structures using a nonlinear fatigue modulus verified from experimental data. These data were based on the degradation of the fatigue modulus, for two directions cells (*L* is the core ribbon direction and *W* is the direction in which the core is expanded). Another study conducted by Hossain and Shivakumar (2014) showed the static and fatigue response in beams using the four-point flexural test of Eco-Core in glass/vinyl ester composite-sheet sandwiches.

Miyano *et al*. (2006) have proposed a method of accelerated testing to predict the life time at fatigue for two kinds of quasi-isotropic CFRP laminates (the first structure was UT500/135 which consists of twill-woven UT500 carbon fiber and the second structure was 135 epoxy resin and T800S/3900-2B which consists of unidirectional T800 carbon fiber and 3900 epoxy resin) subjected to a random combination of frequency, temperature, and stress ratio based on the time–temperature superposition principle. Miyano *et al.* (2008) have presented a new accelerated method to estimate the long-term strength of CFRP laminates for innovative marine under water absorption conditions, at various temperatures and strain rates, for three kinds of CFRP laminates: conventional plain fabric T300 carbon fibers/vinylester, flat yarn plain fabric T700 carbon fibers/vinylester and multi-axial knitted T700 carbon fibers/vinylester. Nakada and Miyano (2009) determined the fatigue life by using accelerated testing methodologies in the marine industry. They tested five kinds of fiber-reinforced polymer (FRP) laminates combined with matrix resin, fiber, and fabric, under water temperatures and environments based on the time-temperature superposition principle. Master curves of the flexural fatigue were plotted for five kinds of FRP laminates, at three conditions of water-absorption that were performed at various temperatures and loading rates.

A study by Rajaneesh *et al.* (2016) covered issues regarding the achievement of accelerated testing methodologies and a behavior analysis of the plain weave 3K carbon-70P/epoxy CFRP laminates using flexural fatigue life. The master curves were constructed for flexural fatigue strength to predict the life of the CFRP laminates using Weibull analysis and the Arrhenius acceleration model.

The objective of this study was to investigate the behavior, in static and fatigue modes, during three-point flexural loading of sandwich structures with CFRP skins and a

balsa wood core. For the static mode, the mechanical characteristics at three-point flexural testing and the impact behavior of CFRP-balsa sandwich structures were determined. Due to these sandwich structures that had presented long-term life during fatigue tests, it was necessary to use accelerated testing methodologies. The methodology proposed in this paper was the accelerated testing of the CFRP-balsa sandwich structures. This involved the extrapolation of the number of cycles from accelerated testing to normal testing, and the determination of the mean life in normal three-point flexural tests.

EXPERIMENTAL

Materials

A series of specimens having a sandwich structure with CFRP skin and a balsa wood core were investigated. The CFRP-balsa sandwich structures tested in this paper can be used for the following applications: ship design (hull, bulkheads), renewable energy (rotor blades), aerospace (small-size aircraft models), and railroad vehicles (floor). The CFRP-balsa sandwich structures were manufactured by bonding layers of 3K plain weave carbon-fiber (Fibre Glast Developments Corp., Brookville, OH, USA) prepreg to each side of an end-grain balsa core. The sandwich structures were cured at high temperatures (120 °C) and under pressure (45 psi), resulting in fully consolidated carbon fiber skins that were completely bonded to the balsa core.

The specimens were cut from a CFRP- balsa sandwich plate to the dimensions 300 mm by 160 mm for the static and fatigue loadings using the three-point flexural test. The sandwich structure skins were made of carbon-fiber plain weave, style 282, and had a prepreg resin content of 44%. The main components of the CFRP-balsa sandwich structures were carbon-fiber plain weaves style, 282, with characteristics as specified in Table 1, resin properties as described in Table 2, and balsa wood properties as described in Table 3.

Table 1. Characteristics of Carbon-fiber Plain Weave, Style 282

Material	Weave	Warp Count	Fill Count	Weight (g/m^2)	Thickness (mm)	Warp Fiber	Fill Fiber
Carbon Fiber, Style 282	Plain Weave	12.5	12.5	195.97	0.25	3K Carbon Standard Modulus PAN	3K Carbon Standard Modulus PAN

Table 2. Neat Resin Properties

Material	Density (g/cm^3)	Moisture Absorption (%)	Tensile Strength (MPa)	Tensile Modulus (GPa)	Tensile Strain	Fracture Toughness ($MPa \cdot m^{1/2}$)
Resin	1.26	7%	49.65	2.89	>9.5%	4.94

Table 3. End-grain Balsa Properties

Material	Density (g/cm^3)	Thickness (mm)	Compressive Strength (MPa)	Compressive Modulus (GPa)	Shear Strength (MPa)	Shear Modulus (GPa)
Balsa	0.16	5.8	0.012	0.004	3	0.00016

Methods

Static flexural test

The specimens of CFRP-balsa sandwich structures were cut from a plate using the Maxiem 1530 Abrasive Waterjet System (Omax Corp., Kent, USA). The specimens were cut to the dimensions of 160 mm x 16 mm x 7 mm, which corresponded to the length, width, and thickness, according to the standard ASTM C393-11 (2011). The three-point flexural tests were conducted on a WDW-150S universal testing machine (Jinan Testing Equipment IE Corporation, Jinan, China) at the loading rate of 6 mm/min. The testing method for the three-point flexure of the specimens determined the shear characteristics both on the faces and in the core of the sandwich structure. This type of test was used in this paper, because the sandwich structures present fractures at relatively small deformations. This method was also used to investigate the mechanical performances of the sandwich structure (the flexural strength, the flexural modulus, and other aspects related to stress, such as displacement). Table 4 describes the dimensional characteristics of the specimens tested at the three-point flexural condition. Ten specimens were subjected to the three-point flexural test and the dimensions of these tested specimens complied with the three requirements of the standard ASTM C393-11 (2011).

Table 4. The Dimensions of Static Flexural Test Specimen

Material	Sandwich Length (*L*) (mm)	Sandwich Thickness (*d*) (mm)	Sandwich Width (*b*) (mm)	Span Length (*S*) (mm)	Core Thickness (*c*) (mm)	Nominal Facing Thickness (*t*) (mm)
CFRP-Balsa	160	6	16	110	5.5	0.25

Figure 2a represents a cross-section of a specimen used in the three-point flexural test. The scheme of the three-point flexural test and the organization mode of the experiments are shown in Fig. 2b.

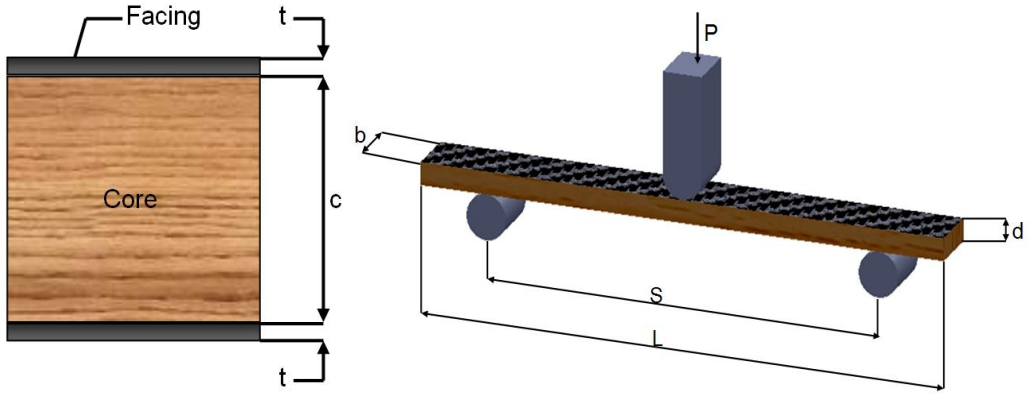

Fig. 2. (a) The definition of the sandwich structure cross-section, and (b) the schematic of the three-point flexural loading set-up

To calculate the core shear (τ), the following equation was used,

$$\tau = \frac{P}{(d + c)b} \quad (1)$$

where P is the force prior to failure (N), d is the sandwich thickness (mm), c is the core thickness (mm), and b is the sandwich width (mm).

To calculate the flexural facing strength (σ), the following equation was used,

$$\sigma = \frac{PS}{2t(d+c)b} \quad (2)$$

where S is the span length (mm) and t is the nominal facing thickness (mm).

Analysis of Charpy impact testing

One of the most important methods for the dynamic testing of sandwich structures through impact is flexural testing on notched and unnotched specimens. During the Charpy impact test, the specimen was placed on the two feet of the hammer frame. The hammer fell from a height of 710 mm by means of a striker made of steel material and struck and broke the specimen, thus consuming part of the kinetic energy of the pendulum. The pendulum rose to a certain height, depending on the material characteristic, using the remaining energy. Energy absorbed during impact test is determined by the difference in the height of the hammer before and after the fracture of specimen. The impact test samples of the sandwich structure were prepared according to the required dimensions as stated in the ISO 179-1 standard (2010) (Table 5).

Table 5. Dimensions of the Charpy Impact Test Specimen

Material	Sandwich Length (*L*) (mm)	Sandwich Thickness (*d*) (mm)	Sandwich Width (*b*) (mm)
CFRP-Balsa	150	6	10

The CFRP-balsa sandwich structures were tested *via* the Charpy flatwise impact, with the hammer striking the specimen from direction 1, as shown in Fig. 3a. The device used for testing the impact on the CFRP-balsa sandwich was the Charpy hammer (Werkstoffprüfmaschinen, Leipzig, Germany) (Fig. 3b). The initial data were: hammer weight, 6.8 kg; length of pendulum, 380 mm; and the initial potential energy, 49 J.

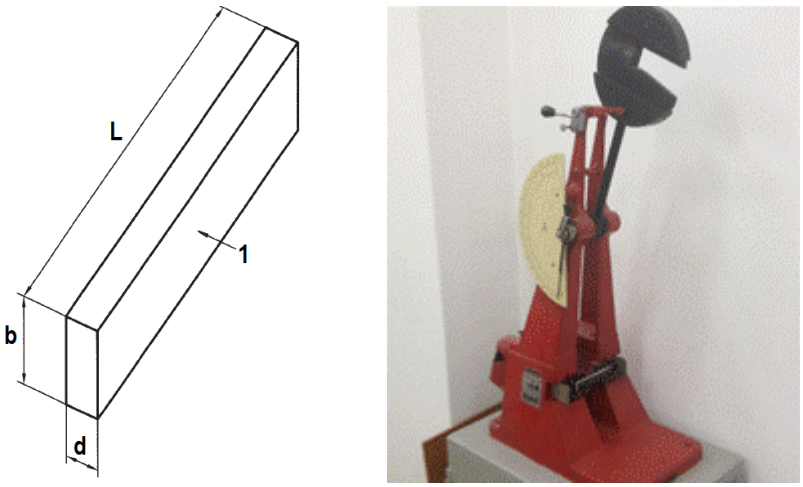

a) b)

Fig. 3. (a) The Charpy flatwise impact specimens, and (b) the schematic of the Charpy impact procedure

For the unnotched specimens, the Charpy impact strength, a_{cU} (kJ/m^2) was determined by the following equation,

$$a_{cU} = \frac{E_c}{d \cdot b} \cdot 10^3 \text{ [kJ/m}^2\text{]} \quad (3)$$

where E_c is the energy (J), absorbed by breaking the CFRP-balsa test specimen; d is the thickness (mm) of the CFRP-balsa test specimen; and b is the width (mm) of the CFRP-balsa test specimen.

Three-point flexural fatigue test

From the perspective of the rising durability of sandwich structures and the increasing demands for quality and reliability, the main difficulty that occurs in normal use tests is the long testing time. The safest and fastest way to validate the durability testing of a sandwich structure is the accelerated fatigue testing technique. The fatigue tests, performed in a dynamic regime, effectively check the fatigue mean life of the sandwich structure through the increased frequency of loading. The testing is accelerated because the stresses are applied with a higher frequency than the normal use frequency, and the ratio between the two frequencies is represented by the acceleration factor.

The fatigue test procedure was conducted according to MIL-STD-401B Sec.5.3 (1967). The CFRP-balsa specimens that were tested at three-point flexural fatigue had dimensions according to this standard (Table 6).

Table 6. The Dimensions of Three-Point Flexural Fatigue Specimens

Material	Sandwich Length (*L*) (mm)	Sandwich Thickness (*d*) (mm)	Sandwich Width (*b*) (mm)
CFRP-balsa	160	6	20

Accelerated fatigue flexural tests were conducted at two frequency levels: 2.5 Hz and 3 Hz. Accelerated flexural fatigue tests were performed under a sinusoidal cyclic load (stress) and a stress ratio of R = 0.1 (a ratio often used in aircraft component testing). Accelerated fatigue data were generated at maximum load level of the static ultimate load. The results were extrapolated for the normal testing levels of 1.5 Hz. At the two accelerated levels (2.5 Hz and 3 Hz), five specimens of CFRP-balsa were tested by the three-point flexural fatigue test (Fig. 4).

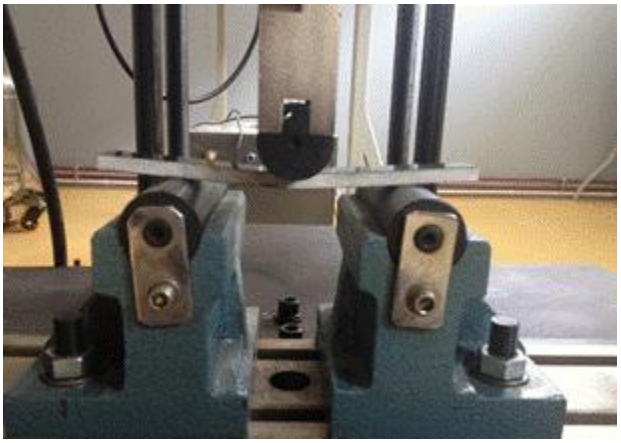

Fig. 4. Three-point flexural fatigue test of the CFRP-balsa sandwich

RESULTS AND DISCUSSION

Mechanical Behavior of the Static Flexural Test

The flexural characteristic curve of load-displacement was constructed by averaging the values that resulted from the 10 CFRP-balsa samples. This curve is shown in graphic form in Fig. 5. The behavior, in terms of load/displacement, of the 10 specimens in static flexural had two main stages. First, linear movement increased between the applied load and the displacement with some nonlinear behavior towards the top of the curve. This was followed by a sudden drop at the maximum load upon the fracture of the specimens. The maximum load, until the time when the irreversible deformation occurred in the material of the sandwich structure, was approximately 140 N. In addition, the deformation that occurred after the irreversible deterioration of the CFRP-balsa sandwich structure material was 3.5 mm.

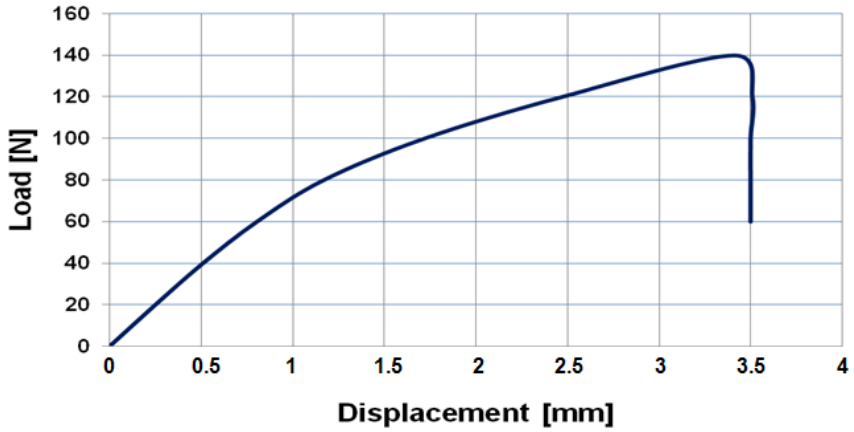

Fig. 5. The load-displacement static flexural behavior of the CFRP-Balsa sandwich specimens

The three-point flexural tests on the sandwich structures allowed the determination of the shear strength of both the core and the faces. Forces prior to failure were determined experimentally on the basis of flexural tests for the 10 specimens tested. The values of forces prior to failure were used in Eqs. 1 and 2 to calculate the core shear strength (τ) and flexural facing strength (σ), as shown in Table 7.

Table 7. Core Shear Strength and Flexural Facing Strength Specific to Three-Point Flexural Testing of the CFRP-Balsa Specimens

Specimen No.	Force Prior to Failure (N)	Core Shear Strength (MPa)	Flexural Facing Strength (MPa)
1	141	0.076	16.858
2	137	0.074	16.380
3	134	0.072	16.021
4	144	0.078	17.217
5	139	0.075	16.619
6	142	0.077	16.978
7	145	0.078	17.336
8	137	0.074	16.380
9	139	0.075	16.619
10	142	0.077	16.978

For the CFRP-balsa sandwich structures, the program of the three-point flexural testing machine allowed for the calculation of mechanical characteristics, such as flexural strength and flexural modulus. As shown in Fig. 6, the flexural strength varied between 24 MPa and 30 MPa, and the flexural modulus stayed within the values of 3 GPa and 6 GPa.

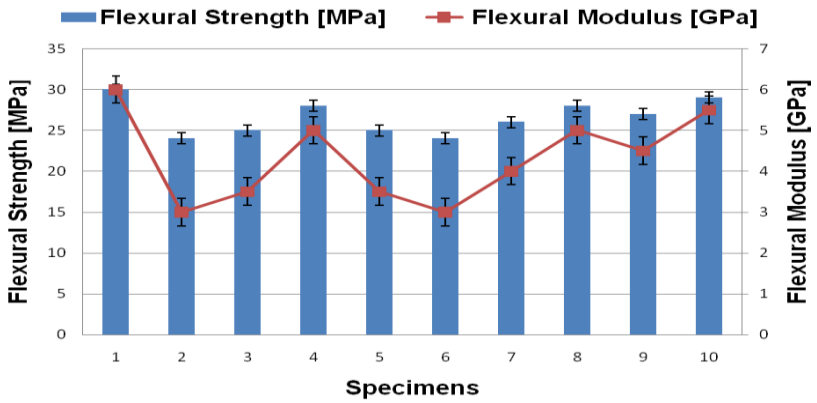

Fig. 6. The flexural strength and flexural modulus of the CFRP-Balsa sandwich specimens

A probability plot was created using Minitab 16 statistical software (Minitab 16, Minitab Ltd, Coventry, UK) for the flexural strength/modulus data of the CFRP-balsa specimens. To verify the normality hypothesis of data for the flexural strength and flexural modulus, the Anderson-Darling statistic test was used. An analysis of Fig. 7 shows that the points representing the data (the values of flexural strength and flexural modulus) were close to the straight line and were included in the 95% confidence interval. These results indicated that the data were normally distributed and the next stage could be precisely processed, verifying data with the Anderson-Darling statistical test. The P value of the Anderson-Darling normality test was 0.541. Both data series (the values of flexural strengths and flexural modulus) passed the Anderson-Darling normality test because they both followed the straight line, and the P values for the normality test were greater than 0.05.

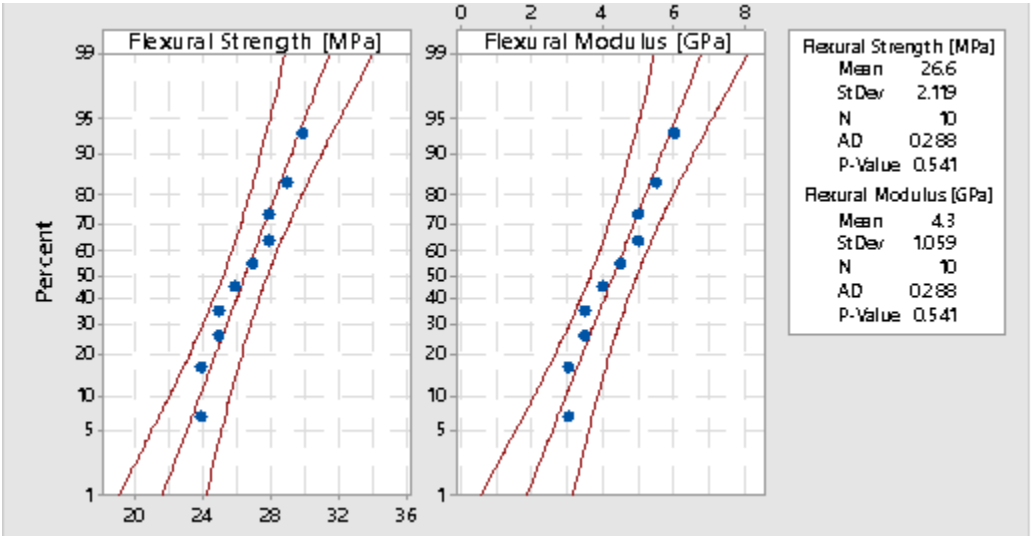

Fig. 7. The probability plot of flexural strength and flexural modulus

The coefficient of variation represents an important numerical characteristic that offers data about the dispersal associated with a random variable, relative to the mean value. A low value of the variation coefficient reflects a low degree of uncertainty of the random variable, whereas a high value of the variation coefficient determines a high degree of uncertainty. In the case studies from the engineering field, usually the value of the variation coefficient has to be between 10% and 30%. Corresponding to the data presented in Table 8, the uncertainty of the two sets of experimental data (flexural strength and flexural modulus) is relatively low and shows the values δ=8% (for flexural strength) and δ=24.6% (for flexural modulus). After the main statistical indicators have been determined (the mean value and the standard deviation), the upper control limit (UCL) and lower control limit (LCL) for flexural strength and flexural modulus were calculated, using the relations 4 and 5.

$$UCL = \hat{\mu} + 3 \cdot \hat{s} \quad (4)$$

$$LCL = \hat{\mu} - 3 \cdot \hat{s} \quad (5)$$

where, $\hat{\mu}$ and $\hat{s}$ represent the estimated values of the parameters of the normal distribution through the moments' method.

Table 8. Statistical Indicators Determined through the Static Three-point Flexural Tests of the CFRP-balsa Specimens

Material	Mean (μ)	Standard deviation (s)	Coefficient of variation (δ) %	Upper control limit (UCL)	Lower control limit (LCL)
CFRP-Balsa – Flexural Strength (MPa)	26.6	2.119	8	32.956	26.361
CFRP-Balsa – Flexural Modulus (GPa)	4.3	1.059	24.6	7.478	3.561

For each tested specimen, the adhesive bonding showed no problems, but the specimens showed some fracture zones over the face of the CFRP-balsa sandwich structure (Fig. 8). The fracture of the sample occurred at the upper skin of the CFRP-balsa specimen, the crack propagated through the entire balsa core and stopped at the lower level, where it caused a debonding of the skin.

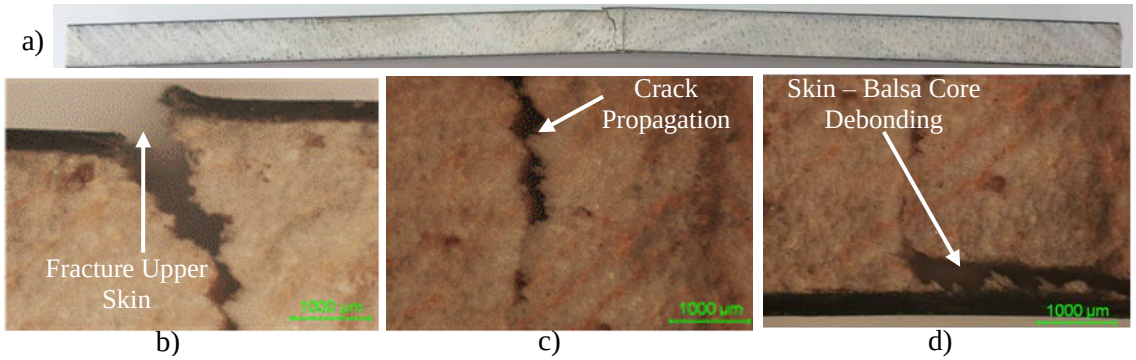

Fig. 8. a) Failure of sandwich panel; the macroscopic aspect (magnification 25X) of the fracture area (b – upper skin, c – balsa core, d – lower skin) of the CFRP-balsa specimens tested with a static three-point flexural mode

Impact Testing Properties of CFRP-Balsa Specimens

The Charpy impact strengths for the 10 CFRP-balsa specimens were determined using Eq. 3. Figure 9 describes the calculated Charpy impact strengths, which were between 40.8 KJ/m^2 and 73.5 KJ/m^2.

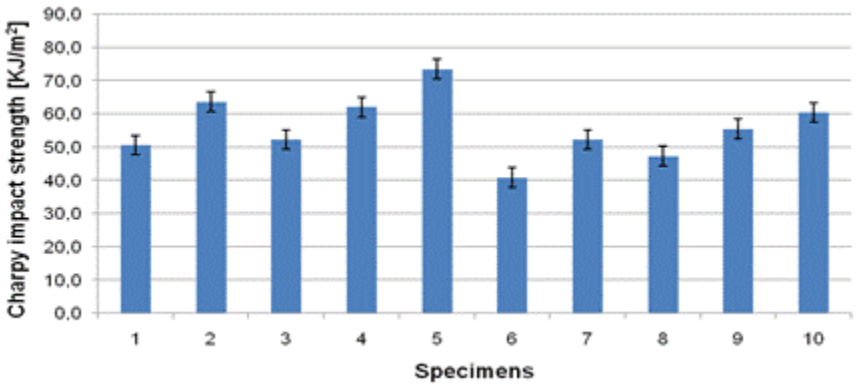

Fig. 9. Charpy impact strengths of the CFRP-Balsa specimens

For the CFRP-balsa specimens tested at impact the main statistical indicators were determined (Table 9). If the variation coefficient (δ) is close to zero (δ < 30%), then the statistical studied data (for strengths at impact the value of δ is 16.7) were homogenous and the mean μ =55.86 was representative for this set of values.

Table 9. Statistical Indicators Determined following the Impact Tests of the CFRP-balsa Specimens

Material	Mean (μ)	Standard deviation (s)	Coefficient of variation (δ)	Upper control limit (UCL)	Lower control limit (LCL)
CFRP-Balsa Impact Strength (KJ/m^2)	55.86	9.332	16.7	83.855	55.359

The 10 specimens that were impact tested had a complete fracture or break (Fig. 10) as a principal deformation mode; thus the results the Charpy impact was calculated were considered valid.

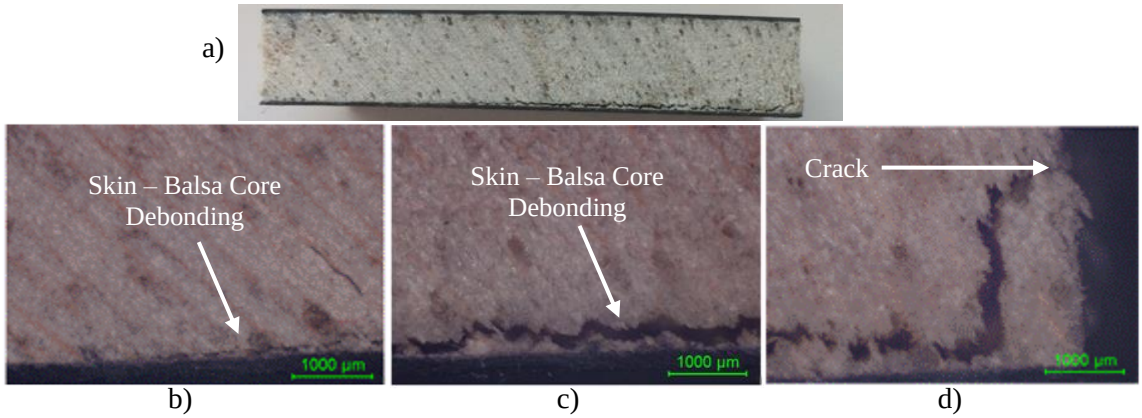

Fig. 10. Failure modes of the CFRP-balsa specimens tested on impact, a) cross section of the specimen; b) and c) skin-balsa core debonding views; d) balsa core cracking (magnification 25X)

The specimens tested at impact presented in the fracture area a crack in the balsa core. The crack propagated and caused a debonding of the upper skin of the sandwich structure (the surface that came into contact first with the Charpy hammer) over a surface of 35 mm.

Accelerated Flexural Fatigue Test

The methodology proposed in this paper consisted of an increased level of flexural testing regime as compared with the normal regime, aimed at accelerated deformation processes of the composite sandwich structures. Such accelerations happened while the same modes, failure mechanisms, and failure structures were maintained. The experimental research was performed on 10 specimens cut from a sheet of CFRP-balsa sandwich structure. The specimens were tested at two levels of accelerated testing (at frequencies of 2.5 Hz and 3 Hz), and the results were extrapolated to the normal test level of 1.5 Hz. In specialty papers (Miyano *et al.* 2006; Miyano *et al.* 2008; Nakada and Miyano 2009; Rajaneesh *et al.* 2016) in the accelerated fatigue tests of the composite structures a frequency value between 1.5 and 2 Hz was used as a normal load regime. Taking into consideration the sandwich structures analysed in this paper and the low performances at mechanical stresses of the balsa wood core, the normal stress level of the load frequency of 1.5 Hz was used.

The statistical processing of the experimental data was performed by an accelerated life testing analysis using ALTA 9 software (ALTA 9 Standard, Reliasoft Corp., Tucson, AZ, USA). To achieve the data extrapolation, a model was used that correlated the life with the accelerated stresses. For the case study in this paper, the Inverse Power Law model and Weibull distribution were suitable. This acceleration model was applied to describe the failure processes, through fatigue, for a wide range of materials, such as plastics, metals, and composites. Equation 4 of the acceleration factor to model the Inverse Power Law and the Weibull distribution is described as follows,

$$F_a = \frac{L_u(V)}{L_a(V)} = \frac{\frac{1}{kV_u^n}}{\frac{1}{kV_a^n}} = \left(\frac{V_a}{V_u}\right)^n \quad (4)$$

where L is the quantifiable life measure (mean life, characteristic life, and median life), V is the stress level, K is the first parameter of the model to be determined ($K > 0$), n is the second parameter to be determined, V_u is the normal stress level, and V_a is the accelerated stress level.

To determine the number of cycles until the failure of the CFRP-balsa specimens (under a normal testing rate at 1.5 Hz frequency), the experimental data that resulted from the accelerated flexural fatigue test were statistically processed. The following parameter values, modelling the Inverse Power Law and Weibull distribution, resulted from the statistical analysis: $\beta = 4.718$, $k = 0.0000005$, and $n = 4.239$. The acceleration factor that corresponded to the modelling of the Inverse Power Law and Weibull distribution was calculated with Eq. 4, and was determined for each level of frequency acceleration. Considering the multiplication between the number of cycles until failure in accelerated conditions and the calculated values of acceleration factors, the number of cycles until failure in normal testing conditions (Table 10) was determined for the CFRP-balsa specimens.

Table 10. Determination of the Number of Cycles until Failure for the Normal Level Testing (1.5 Hz frequency) of the CFRP-Balsa Specimens

Specimen No.	No. Cycles Until Failure (accelerated conditions)	Accelerated Frequency Level (Hz)	Acceleration Factor	No. Cycles Until Failure (normal conditions)
1	30056	2.5	8.72222	262155
2	34536			301231
3	37576			327746
4	44678			389691
5	55672			485583
6	12087	3	18.89521	228386
7	14065			265761
8	19983			377583
9	21898			413767
10	24567			464199

The main objective of the accelerated fatigue tests was to determine the mean fatigue life in the normal testing regime. The data from the accelerated tests were used to estimate the mean number of cycles until failure of the CFRP-balsa specimens in the normal level testing regime (1.5 Hz). Figure 11 shows the principle according to which the accelerated tests were performed and the two levels of accelerated stress (2.5 Hz to 3 Hz).

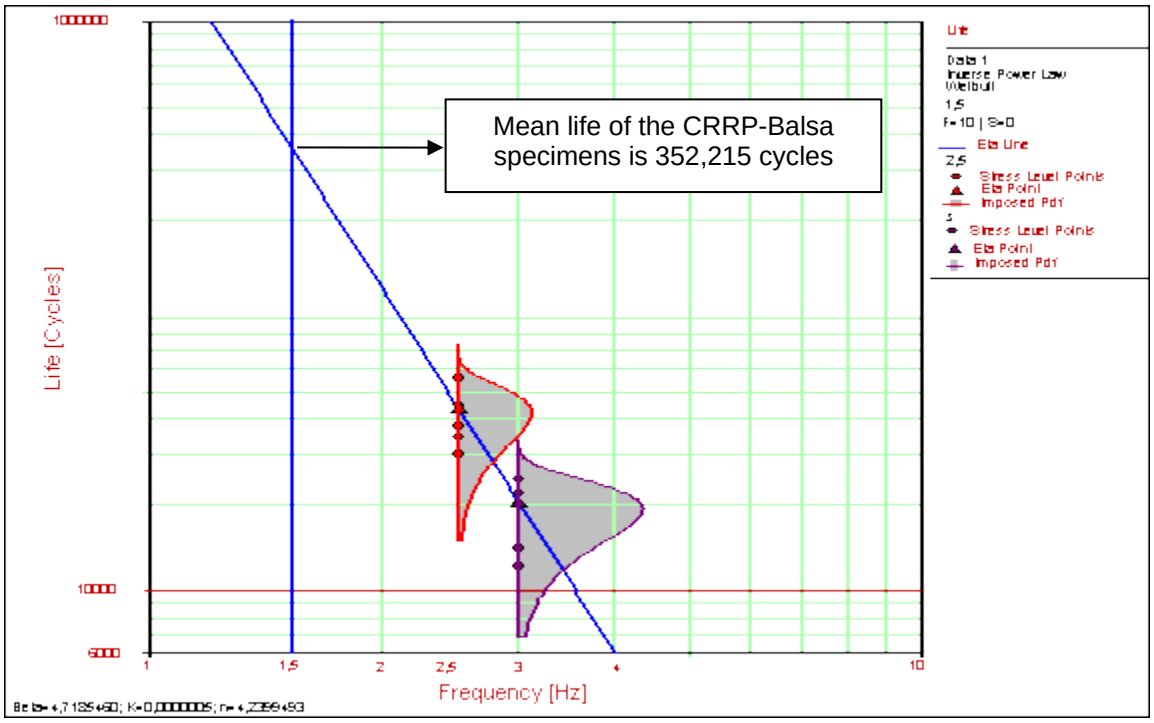

Fig. 11. The determination of the mean fatigue life by the graphical method of the CFRP-balsa specimens

By relating the acceleration to the modelling of the Power Law and Weibull distribution, the results could be extrapolated from the accelerated level to the normal test level. The results were extrapolated by determining the mean cycle values for the two levels of accelerated stress (at 2.5 Hz and 3 Hz). A straight line was plotted through these

points. Lastly, the line was extended up to the normal level test (1.5 Hz) and the mean life in the normal testing level of the CFRP-balsa specimens was determined.

The mean number of cycles until failure in the normal test regime was determined analytically and graphically. The analytical estimation of the mean number of cycles was based on the well-known relationship of the reliability indicator (also called the adequate mean) to the acceleration model of Inverse Power Law and Weibull distribution. To estimate the mean, the graphic method and the extrapolation algorithm of the results mentioned above were used, and the resulting mean number of cycles until failure in the normal test level (frequency 1.5 Hz) was 352,000.

The scope of the fatigue tests was to obtain knowledge on the fatigue behavior of the CFRP-balsa specimens tested by determining the S-N diagram and the failure modes. The fatigue behavior was similar to the 10 CFRP-balsa specimens, and it followed a linear trend of decreasing the maximum stress proportional to the increase in the number of cycles until failure. The mean number of cycles until failure under normal test conditions (1.5 Hz frequency and stress ratio R = 0.1) was represented graphically according to the maximum stress at which the CFRP-balsa specimens failed, multiplied by the acceleration factor. This curve represented the flexural fatigue curve of the CFRP-balsa specimens (Fig. 12).

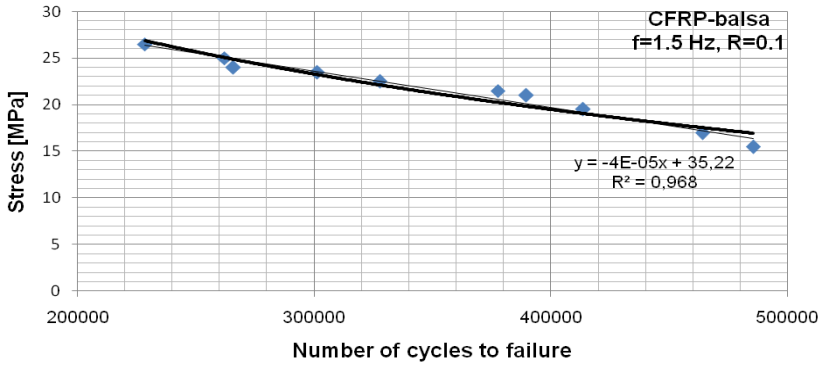

Fig. 12. Flexural fatigue S-N curve of the CFRP-balsa specimens

The macrostructural analyses were performed using a Nikon Eclipse MA 100 optical microscope (Nikon, Tokyo, Japan). The bonding of the CFRP skin to the balsa core plays an essential role in the realization and the fatigue testing of a sandwich type composite structure. With the increase in the number of cycles of fatigue testing of the CFRP-balsa specimens, comes an active phase, during which the cracks of the skin and then the debondings of the core, that start especially from the edges or from inside, occur. The cause of the onset of debondings or delaminations in the immediate vicinity of the cracks of the sandwich structures is the complex tridimensional state of tensions, produced by the local load redistributions. For the accelerated fatigue tests the CFRP-balsa specimens present four distinct phases before the total fracture (Fig. 13). The first phase consists of the debonding of the skin in the middle area of the sample, where the force was applied, on the upper skin that is subjected to compression. A second phase consists of the onset of the crack of the balsa core and the subsequent propagation of the crack to the lower skin. During this phase the crack has also caused a 12-mm debonding on the surface of the upper skin. A third phase consists of the debonding of the lower skin of the sandwich structure over a 61-mm distance.

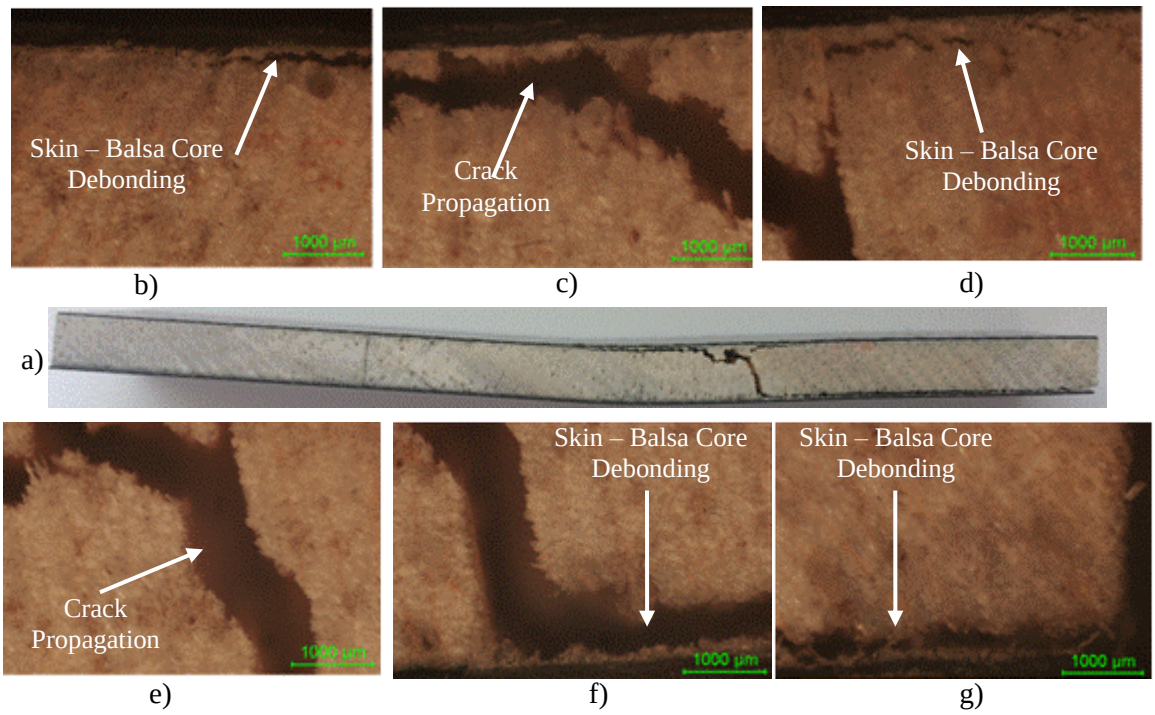

Fig. 13. Macroscopic views (magnification 25X) of the crack propagation during the accelerated flexural fatigue test of the CFRP-balsa specimen, a) failure mode of specimen; b) upper skin – balsa core debonding; c) crack propagation of the balsa core; d) upper skin – balsa core debonding; e) crack propagation of the balsa core; f) and g) lower skin – balsa core debonding

CONCLUSIONS

1. The acceleration and extrapolation methodology for the normal testing allowed the characterization of the fatigue behavior and the determination of the mean fatigue life of the CFRP-balsa sandwich structures.
2. Using the methodology of acceleration testing, the S-N fatigue life curve of the CFRP-balsa specimens was predicted under three-point flexural testing.
3. The cumulative number of cycles until failure from the accelerated tests was 295,000, and the sum of the number of cycles until failure in normal testing conditions was 3,516,000. Consequently, the primary purpose of performing accelerated tests on the CFRP-balsa specimens was confirmed, namely, to reduce the number of times until failure using the accelerated tests. By implementing the accelerated testing methodologies on the CFRP-balsa specimens, the number of cycles until failure was reduced by 11.9 times.
4. The three-point flexural testing of the CFRP-balsa sandwich structures determined the following mechanical characteristics: the flexural strength, the flexural modulus, the core shear strength, and the flexural facing strength.
5. Using the Charpy impact test, the mean impact strength for the 10 CFRP-balsa specimens was determined to be 55.9 KJ/m2.
6. The CFRP-balsa specimens tested at flexural in a static regime presented a fracturing of the upper skin, with a propagation of the crack to the lower skin, causing its debonding. In reference to the behaviour of the CFRP-balsa specimens tested at

impact, a crack in the balsa core was observed; this determined a debonding of the upper skin. Analysis of the results obtained from the accelerated fatigue tests revealed that the debonding occurred at the upper skin of the sandwich structure, followed by the crack of the entire balsa core and eventually by the debonding of the lower skin.

ACKNOWLEDGMENTS

The authors acknowledge the structural founds project PRO-DD (POS-CCE. O.2.2.1., ID 123. SMIS 2637. Ctr. No. 11/2009) for providing the infrastructure used in this work.

REFERENCES CITED

Abbadi, A., Azari, Z., Belouettar, S., Gilgert, J., and Freres, P. (2010). "Modelling the fatigue behaviour of composites honeycomb materials (aluminum/aramide fibre core) using four-point bending tests," *International Journal of Fatigue* 32(11), 1739-1747. DOI: 10.1016/j.ijfatigue.2010.01.005

ASTM C393-11 (2011). "Flexural properties of flat sandwich constructions," ASTM International, West Conshohocken, PA.

Atas, C., and Sevim, C. (2010). "On the impact response of sandwich composites with cores of Balsa wood and PVC foam," *Composite Structures* 93(1), 40-48. DOI: 10.1016/j.compstruct.2010.06.018

Borrega, M., and Gibson, L. J. (2015). "Mechanics of balsa (*Ochroma pyramidale*) wood," *Mechanics of Materials* 84, 75-90. DOI: 10.1016/j.mechmat.2015.01.014

Boukharouba, W., Bezazi, A., and Scarpa, F. (2014). "Identification and prediction of cyclic fatigue behaviour in sandwich panels," *Measurement* 53, 161-170. DOI: 10.1016/j.measurement.2014.03.041

Chemami, A., Bey, K., Gilgert, J., and Azari, Z. (2012). "Behavior of composite sandwich foam-laminated glass/epoxy under solicitation static and fatigue," *Composites Part B- Engineering* 43(3), 1178-1184. DOI: 10.1016/j.compositesb.2011.11.051

Chen, A., Kim, H., Asaro, R. J., and Bezares, J. (2011). "Non-explosive simulated blast loading of balsa core sandwich composite beams," *Composite Structures* 93(11), 2768-2784. DOI: 10.1016/j.compstruct.2011.05.027

Da Silva, A., and Kyriakides, S. (2007). "Compressive response and failure of balsa wood," *International Journal of Solids and Structures* 44(25-26), 8685-8717. DOI: 10.1016/j.ijsolstr.2007.07.003

Harris, B. (2003). *Fatigue in Composites, 1st Edition*, Woodhead Publishing, Cambridge, UK.

Hossain, M. M., and Shivakumar, K. (2014). "Flexural fatigue failures and lives of Eco-Core sandwich beams," *Materials & Design* 55, 830-836. DOI: 10.1016/j.matdes.2013.09.022

ISO 179-1 (2010). "Plastics - Determination of Charpy impact properties," International Organization for Standardization, Geneva, Switzerland.

Jover, N., Shafiq, B., and Vaidya, U. (2014). "Ballistic impact analysis of Balsa core sandwich composites," *Composites Part B- Engineering* 67, 160-169. DOI: 10.1016/j.compositesb.2014.07.002

Kandare, E., Luangtriratana, P., and Kandola, B. K. (2014). "Fire reaction properties of flax/epoxy laminates and their Balsa-core sandwich composites with or without fire protection," *Composites Part B- Engineering* 56, 602-610. DOI: 10.1016/j.compositesb.2013.08.090

Kotlarewski, N. J., Ozarska, B., and Gusamo, B. K. (2014). "Thermal conductivity of Papua New Guinea Balsa wood measured using the needle probe procedure," *BioResources* 9(4), 5784-5793. DOI: 10.15376/biores.9.4.5784-5793

Li, J. H., Hunt, J. F., Gong, S. Q., and Cai, Z. Y. (2014). "High strength wood-based sandwich panels reinforced with fiberglass and foam," *BioResources* 9(2), 1898-1913. DOI: 10.15376/biores.9.2.1898-1913

Midgley, S., Blyth, M., Howcroft, N., Midgley, D., and Brown, A. (2010). *Balsa: Biology, Production and Economics in Papua New Guinea* (Report No. 73), Australian Centre for International Agricultural Research, Canberra, Australia.

Miyano, Y., Nakada, M., and Nishigaki, K. (2006). "Prediction of long-term fatigue life of quasi-isotropic CFRP laminates for aircraft use," *International Journal of Fatigue* 28(10), 1217-1225. DOI: 10.1016/j.ijfatigue.2006.02.007

Miyano, Y., Nakada, M., Ichimura, J., and Hayakawa, E. (2008). "Accelerated testing for long-term strength of innovative CFRP laminates for marine use," *Composites Part B: Engineering*, 39(1), 5-12. DOI: 10.1016/j.compositesb.2007.02.009

MIL-STD-401B (1967). "Sandwich constructions and core materials; General test methods," Department of Defense, Washington, D. C.

Nakada, M., and Miyano,Y. (2009). "Accelerated testing for long-term fatigue strength of various FRP laminates for marine use," *Composites Science and Technology* 69(6), 805-813. DOI: 10.1016/j.compscitech.2008.02.030

Osei-Antwi, M., De Castro, J., Vassilopoulos, A. P., and Keller, T. (2014). "Analytical modelling of local stresses at balsa/timber core joints of FRP sandwich structures," *Composite Structures* 116, 501-508. DOI: 10.1016/j.compstruct.2014.05.050

Rajaneesh, A., Satrio, W., Chai, G. B., and Sridhar, I. (2016). "Long-term life prediction of woven CFRP laminates under three point flexural fatigue," *Composites Part B-Engineering* 91, 539-547. DOI: 10.1016/j.compositesb.2016.01.028

Toson, B., Viot, P., and Pesqué, J. J. (2014). "Finite element modeling of balsa wood structures under severe loading," *Engineering Structures* 70, 36-52. DOI: 10.1016/j.engstruct.2014.03.017

Vinson, J. R. (1999). *The Behavior of Sandwich Structures of Isotropic and Composite Materials*, CRC Press, Boca Raton, FL, USA.

Article submitted: October 30, 2016; Peer review completed: December 29, 2016;
Revised version received and accepted: February 9, 2017; Published: February 21, 2017.
DOI: 10.15376/biores.12.2.2673-2689